Searching for anisotropy of PTA SGWB correlated with large scale structure with a template-based method

Yun Fang (方芸)

Institute of Fundamental Physics and Quantum Technology,
Ningbo University

based on: **Y. Fang**, Sci.China Phys.Mech.Astron. (2026)

Y. Fang+, in preparation

pulsar redshift:

$$z_a(t) = \sum_A \int \mathrm{d}f \int \mathrm{d}\mathbf{n}\; F_a^A(\mathbf{n})\, h_A(f,\mathbf{n})\, e^{2\pi i f t} \left[1 - e^{-2\pi i f L_a(1+\mathbf{n}\cdot\boldsymbol{p}_a)}\right]$$

timing residual:

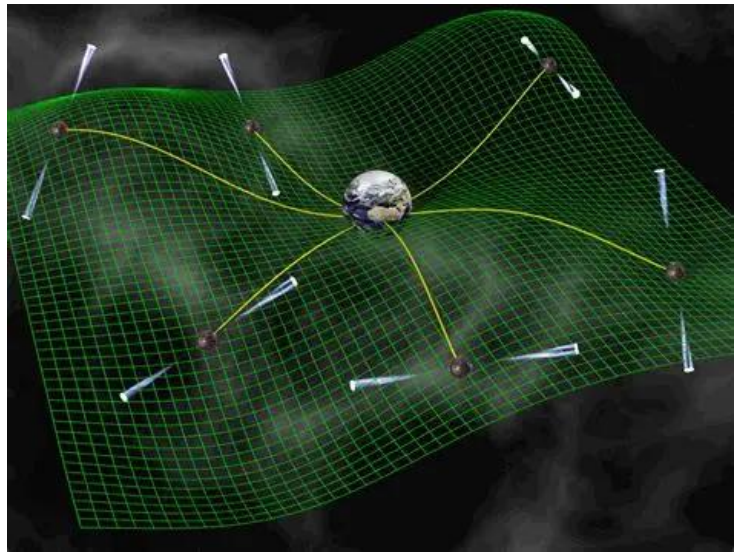
$$r_a(t) = \int^t dt'\, z_a(t')$$

given SGWB:

$$\langle h_A(f,\mathbf{n}) h^*_{A'}(f',\mathbf{n}')\rangle = \frac{1}{2}\,\delta_{AA'}\,\delta(f-f')\,\delta^2(\mathbf{n},\mathbf{n}')\,S_h(f)\,P(\mathbf{n})$$

Cross-spectrum of the residuals:

$$\langle \tilde{r}_a(f)\tilde{r}^*_b(f')\rangle = \frac{1}{2}\delta(f-f')\,\Gamma_{ab}(f)\frac{S_h(f)}{12\pi^2 f^2}$$



HD curve (Hellings & Downs 1983)

pulsar redshift:

$$z_a(t) = \sum_A \int \mathrm{d}f \int \mathrm{d}\mathbf{n}\, F_a^A(\mathbf{n})\, h_A(f,\mathbf{n})\, e^{2\pi i f t} \left[1 - e^{-2\pi i f L_a(1+\mathbf{n}\cdot\boldsymbol{p}_a)}\right]$$

timing residual:

$$r_a(t) = \int^t dt'\, z_a(t')$$

given SGWB:

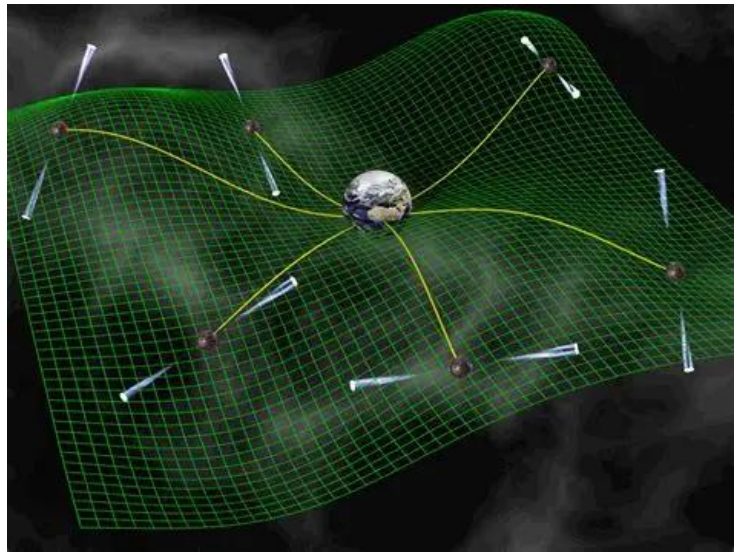
$$\langle h_A(f,\mathbf{n}) h^*_{A'}(f',\mathbf{n}')\rangle = \frac{1}{2}\,\delta_{AA'}\,\delta(f-f')\,\delta^2(\mathbf{n},\mathbf{n}')\,S_h(f)\,P(\mathbf{n})$$

Cross-spectrum of the residuals:

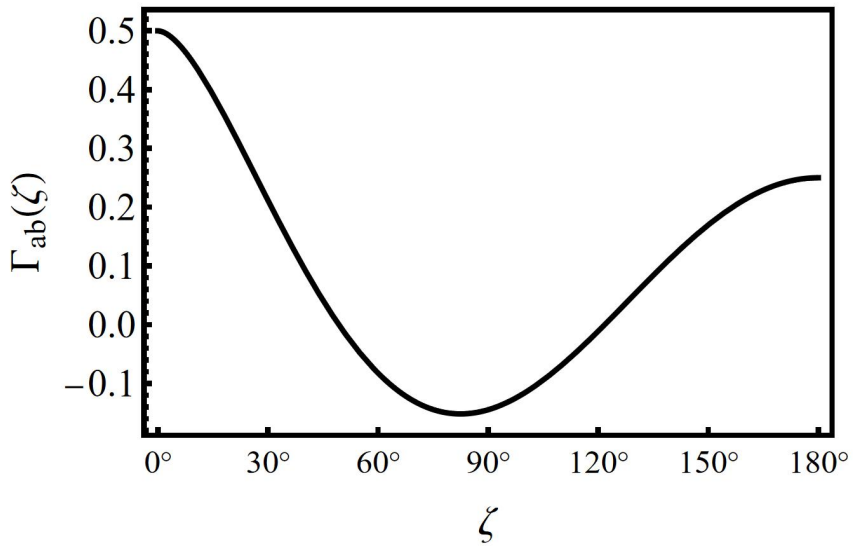
$$\langle \tilde{r}_a(f)\tilde{r}^*_b(f')\rangle = \frac{1}{2}\delta(f-f')\,\Gamma_{ab}(f)\frac{S_h(f)}{12\pi^2 f^2}$$

ORF: $\Gamma_{ab}(\zeta) = \frac{3}{2}\sum_A \int \mathrm{d}\mathbf{n}\, F_a^A(\mathbf{n}) F_b^A(\mathbf{n})\, P(\mathbf{n})$

Isotropic SGWB: $P(n) = 1$



HD curve (Hellings & Downs 1983)



pulsar redshift:

$$z_a(t) = \sum_A \int \mathrm{d}f \int \mathrm{d}\mathbf{n}\, F_a^A(\mathbf{n})\, h_A(f,\mathbf{n})\, e^{2\pi i f t} \left[1 - e^{-2\pi i f L_a(1+\mathbf{n}\cdot\boldsymbol{p}_a)}\right]$$

timing residual:

$$r_a(t) = \int^t dt'\, z_a(t')$$

given SGWB:

$$\langle h_A(f,\mathbf{n}) h^*_{A'}(f',\mathbf{n}')\rangle = \frac{1}{2}\,\delta_{AA'}\,\delta(f-f')\,\delta^2(\mathbf{n},\mathbf{n}')\,S_h(f)\,P(\mathbf{n})$$

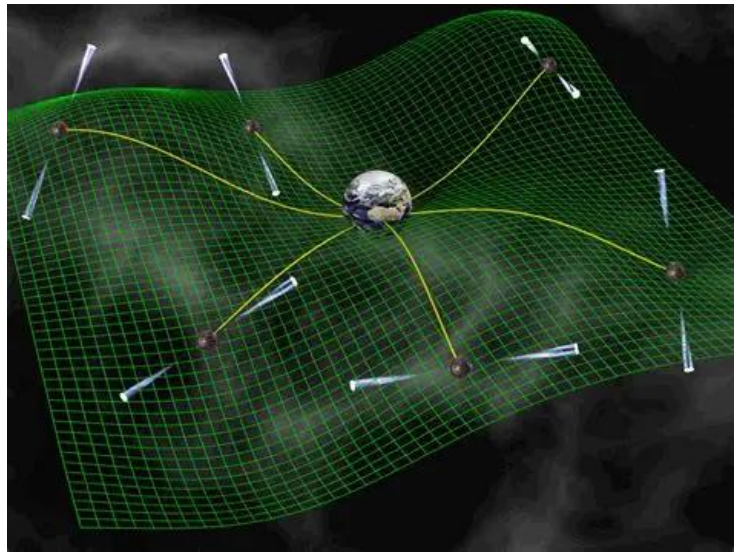
Cross-spectrum of the residuals:

$$\langle \tilde{r}_a(f)\tilde{r}^*_b(f')\rangle = \frac{1}{2}\delta(f-f')\,\Gamma_{ab}(f)\frac{S_h(f)}{12\pi^2 f^2}$$

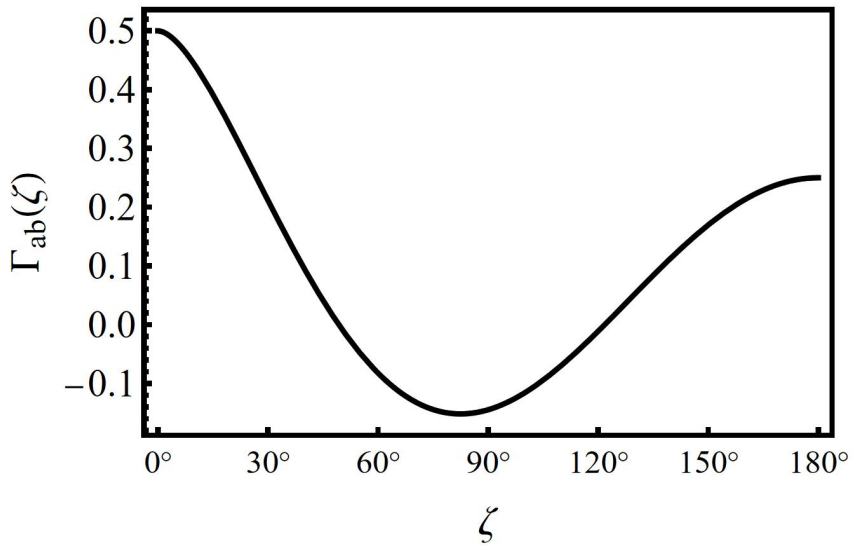
ORF: $\Gamma_{ab}(\zeta) = \frac{3}{2}\sum_A \int \mathrm{d}\mathbf{n}\, F_a^A(\mathbf{n}) F_b^A(\mathbf{n})\, P(\mathbf{n})$

Isotropic SGWB: $P(n) = 1$

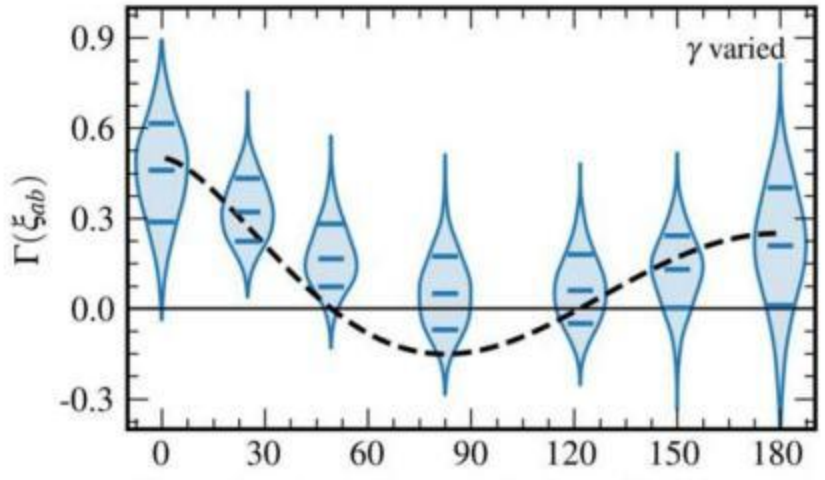
Anisotropic SGWB: $P(\mathbf{n}) = \sum_{\ell m} c_{\ell m} Y_{\ell m}(\mathbf{n})$

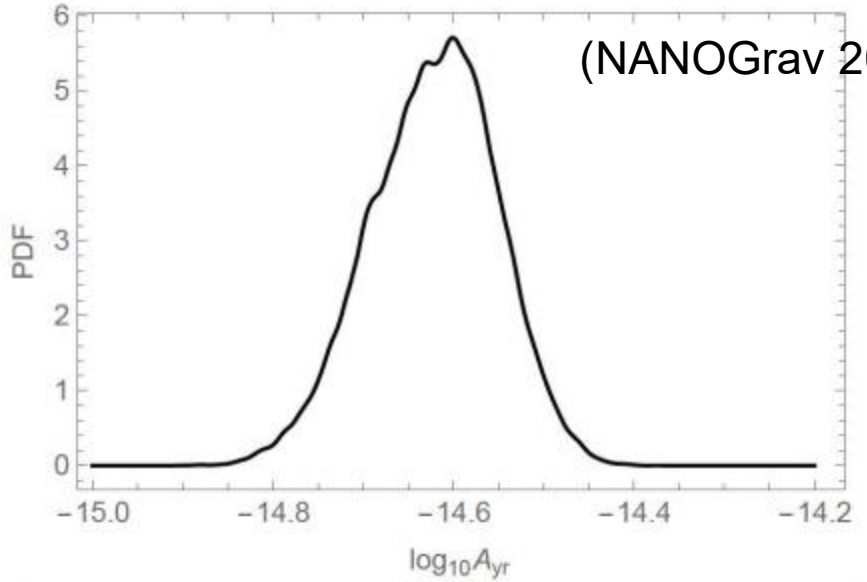


HD curve (Hellings & Downs 1983)

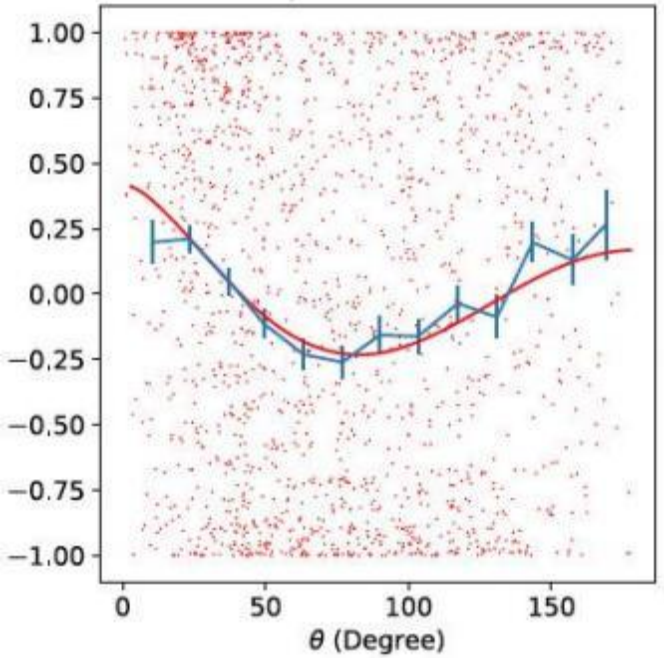


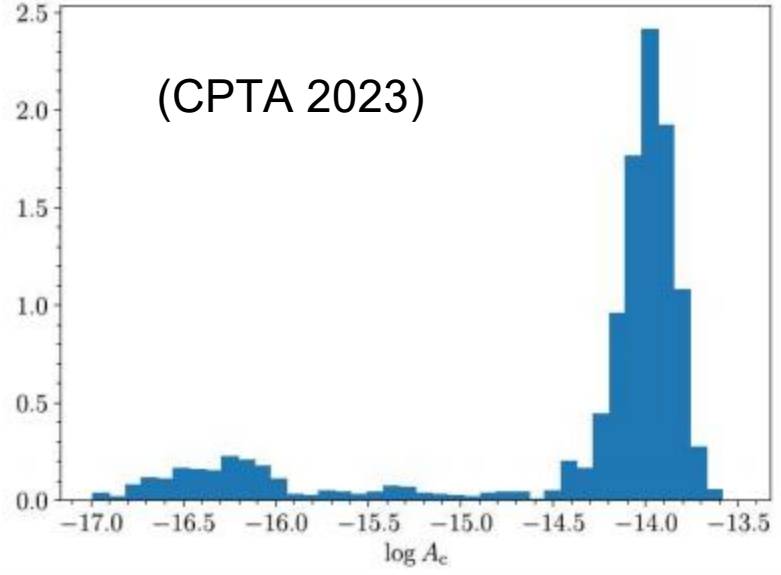
Evidence of PTA SGWB





(NANOGrav 2023)





(CPTA 2023)

Anisotropy probes the origin of the PTA SGWB

The spectrum alone may not distinguish the underlying sources.

ORIGINS

Supermassive black hole binaries

Inspiralling binaries composed of SMBHs contribute to the nanohertz background.

(Phinney 2001; Jaffe & Backer 2003; Sesana 2013; Agazie et al. 2023; Bi et al. 2023)

Early-Universe processes

Cosmic strings, phase transitions or primordial fluctuations.

(Kosowsky et al.1992; Caprini & Figueroa 2018; Ellis & Lewicki 2021; Afzal et al. 2023)

A connection to large-scale structure

- An SMBHB background naturely trace the galaxy distribution.
- Cosmological backgrounds can reflect primordial fluctuations and need not trace the galaxy distribution.

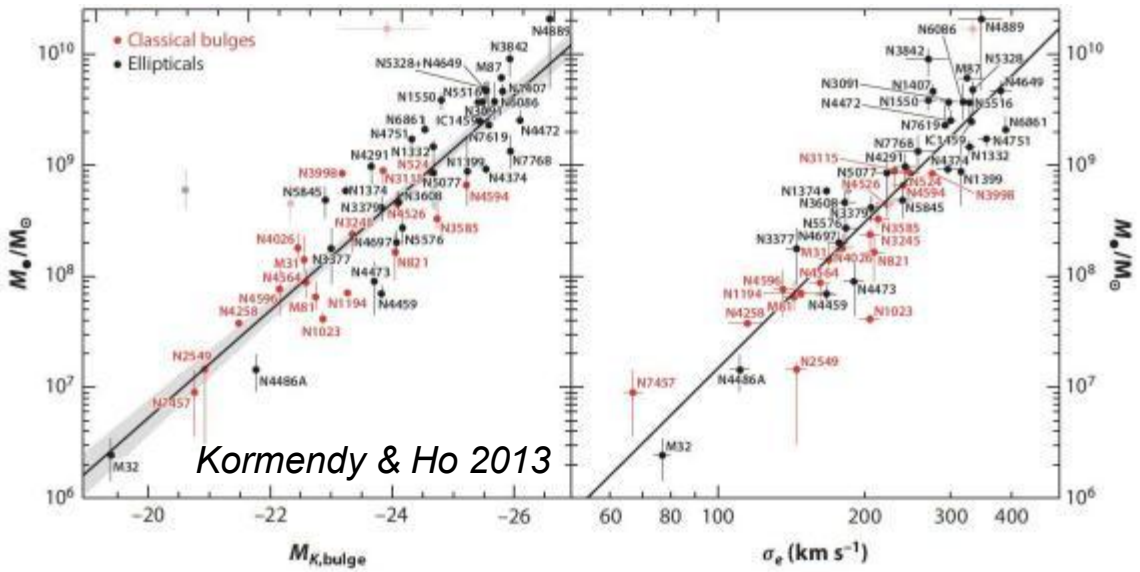
Combine spectral and angular information to constrain the origin.

SMBHs reside in the center of galaxies

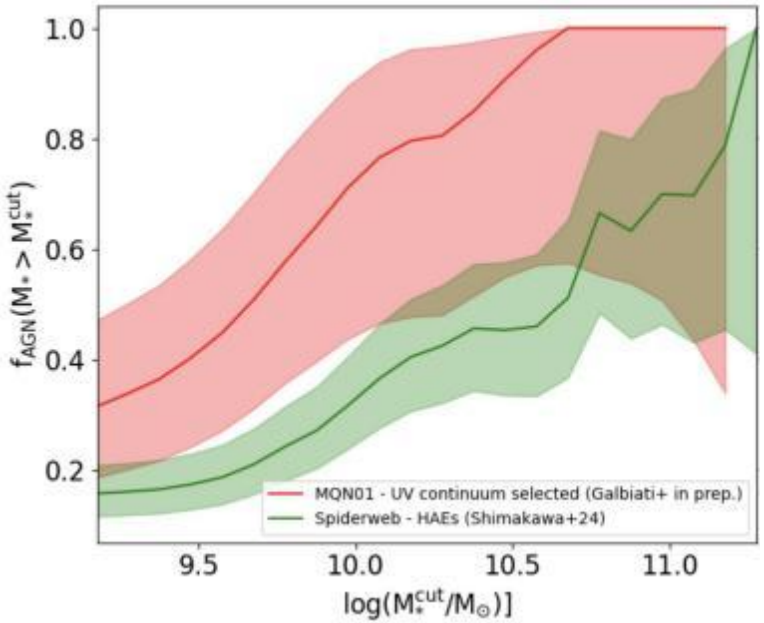
- SMBHs universally reside in the nucleus of most galaxies
  (Magorrian et al. 1998, Ghez et al. 2010; McConnell & C.-P. Ma 2013; EHT Collaboration 2019, 2022)
- Cosmological Large Scale Structure and SMBHs

Scaling relations between SMBHs, galaxies, and halos *(Dressler, 1989; Kormendy 1993; Magorrian et al. 1998; Ferrarese & Merritt 2000; Gebhardt et al. 2000; Kormendy & Ho 2013)*

Massive SMBHs trend to reside in overdense environments *(Travascio et al. 2025; Hellwing et al. 2021)*



$M_{BH}-L_{bulge}$ $M_{BH}-\sigma_*$



Galaxy–GW cross-correlation and the PTA ORF

Linear-scale GW fluctuations in a redshift bin follow:

$$\delta_{\rm GW}(\hat{n}, z) = c(z)\delta_g(\hat{n}, z)$$

Galaxy–GW cross-correlation and the PTA ORF

Linear-scale GW fluctuations in a redshift bin follow:

$$\delta_{\rm GW}(\hat{n}, z) = c(z)\delta_g(\hat{n}, z)$$

Galaxy–GW cross-spectrum:

$$C_\ell^{g_i \rm GW} = \frac{1}{2\ell+1} \sum_{m=-\ell}^{\ell} a_{\ell m}^{g_i} a_{\ell m}^{\rm GW\,*} = c(z_i) \frac{1}{2\ell+1} \sum_m |a_{\ell m}^{g_i}|^2$$

Galaxy–GW cross-correlation and the PTA ORF

Linear-scale GW fluctuations in a redshift bin follow:

$$\delta_{\rm GW}(\hat{n},z) = c(z)\delta_g(\hat{n},z)$$

Galaxy–GW cross-spectrum:

$$C_\ell^{g_i{\rm GW}} = \frac{1}{2\ell+1}\sum_{m=-\ell}^{\ell} a_{\ell m}^{g_i} a_{\ell m}^{{\rm GW}\,*} = c(z_i)\frac{1}{2\ell+1}\sum_m |a_{\ell m}^{g_i}|^2$$

Pulsar-pair cross-correlation:

$$\Gamma_{ab} = \Gamma_{ab}^{\rm HD} + \frac{3}{8\pi}\int d\hat{n}\,\delta_{\rm GW}(\hat{n}) \sum_{A=+,\times} F_a^A(\hat{n}) F_b^A(\hat{n})$$

$$= \Gamma_{ab}^{\rm HD} + \varepsilon_i \sum_{\ell m} a_{\ell m}^{g_i} G_{\ell m}^{ab}$$

(Y. Fang, SCPMA 2026)

where $G_{\ell m}^{ab} = \int d\hat{n}\, Y_{\ell m}(\hat{n}) \sum_{A=+,\times} F_a^A(\hat{n}) F_b^A(\hat{n})$ $\qquad \varepsilon_i = \frac{3}{8\pi} c(z_i)$

Galaxy–GW cross-correlation and the PTA ORF

Linear-scale GW fluctuations in a redshift bin follow:

$$\delta_{\rm GW}(\hat{n},z) = c(z)\delta_g(\hat{n},z)$$

Galaxy–GW cross-spectrum:

$$C_\ell^{g_i{\rm GW}} = \frac{1}{2\ell+1}\sum_{m=-\ell}^{\ell} a_{\ell m}^{g_i} a_{\ell m}^{{\rm GW}\,*} = c(z_i)\frac{1}{2\ell+1}\sum_m |a_{\ell m}^{g_i}|^2$$

Pulsar-pair cross-correlation:

$$\Gamma_{ab} = \Gamma_{ab}^{\rm HD} + \frac{3}{8\pi}\int d\hat{n}\,\delta_{\rm GW}(\hat{n}) \sum_{A=+,\times} F_a^A(\hat{n}) F_b^A(\hat{n})$$

$$= \Gamma_{ab}^{\rm HD} + \varepsilon_i \sum_{\ell m} a_{\ell m}^{g_i} G_{\ell m}^{ab}$$

(Y. Fang, SCPMA 2026)

where $G_{\ell m}^{ab} = \int d\hat{n}\, Y_{\ell m}(\hat{n}) \sum_{A=+,\times} F_a^A(\hat{n}) F_b^A(\hat{n})$ $\qquad \varepsilon_i = \frac{3}{8\pi} c(z_i)$

Equivalently, a positive galaxy–SGWB cross-correlation implies an LSS-projected contribution to the cross-correlations between PTA pulsars.

Galaxy–GW cross-correlation and the PTA ORF

Linear-scale GW fluctuations in a redshift bin follow:

$$\delta_{\rm GW}(\hat{n},z) = c(z)\delta_g(\hat{n},z)$$

Galaxy–GW cross-spectrum:

$$C_\ell^{g_i{\rm GW}} = \frac{1}{2\ell+1}\sum_{m=-\ell}^{\ell} a_{\ell m}^{g_i} a_{\ell m}^{{\rm GW}\,*} = c(z_i)\frac{1}{2\ell+1}\sum_m |a_{\ell m}^{g_i}|^2$$

Pulsar-pair cross-correlation:

$$\Gamma_{ab} = \Gamma_{ab}^{\rm HD} + \frac{3}{8\pi}\int d\hat{n}\,\delta_{\rm GW}(\hat{n}) \sum_{A=+,\times} F_a^A(\hat{n}) F_b^A(\hat{n})$$

ORF

$$= \Gamma_{ab}^{\rm HD} + \varepsilon_i \sum_{\ell m} a_{\ell m}^{g_i} G_{\ell m}^{ab}$$

(Y. Fang, SCPMA 2026)

where $G_{\ell m}^{ab} = \int d\hat{n}\, Y_{\ell m}(\hat{n}) \sum_{A=+,\times} F_a^A(\hat{n}) F_b^A(\hat{n})$ $\qquad \varepsilon_i = \frac{3}{8\pi} c(z_i)$

Equivalently, a positive galaxy–SGWB cross-correlation implies an LSS-projected contribution to the cross-correlations between PTA pulsars.

MAP reconstruction of LSS sky map

—— example from 2MPZ galaxy catalog *(Bilicki et al. 2014; Y. Fang, SCPMA 2026)*

$$\delta(p) = \begin{cases} \dfrac{N(p) - \bar{N}}{\bar{N}}, & M_{\rm bin}(p) = 1, \\ 0, & M_{\rm bin}(p) = 0. \end{cases} \qquad M_{\rm bin}(\mathbf{n}) = \begin{cases} 1, & |b(\mathbf{n})| \geq b_{\rm cut}, \\ 0, & \text{otherwise}, \end{cases} \qquad M_{\rm apod}(\mathbf{n}) \equiv \text{Apodize}\left[M_{\rm bin}(\mathbf{n});\, \theta_{\rm apod},\, \text{C1}\right]$$

$$\delta_{\rm used}(p) \equiv \delta(p) - \sum_{k=1}^{4} \beta_k\, B_k(p), \qquad p \in \{p\,:\, M_{\rm apod}(p) > \tau\}$$

$$\delta_{\rm used}(\hat{\boldsymbol{n}}) \approx \sum_{\ell=2}^{\ell_{\rm max}} \sum_{m=-\ell}^{\ell} a_{\ell m}\, Y_{\ell m}(\hat{\boldsymbol{n}})\,,$$

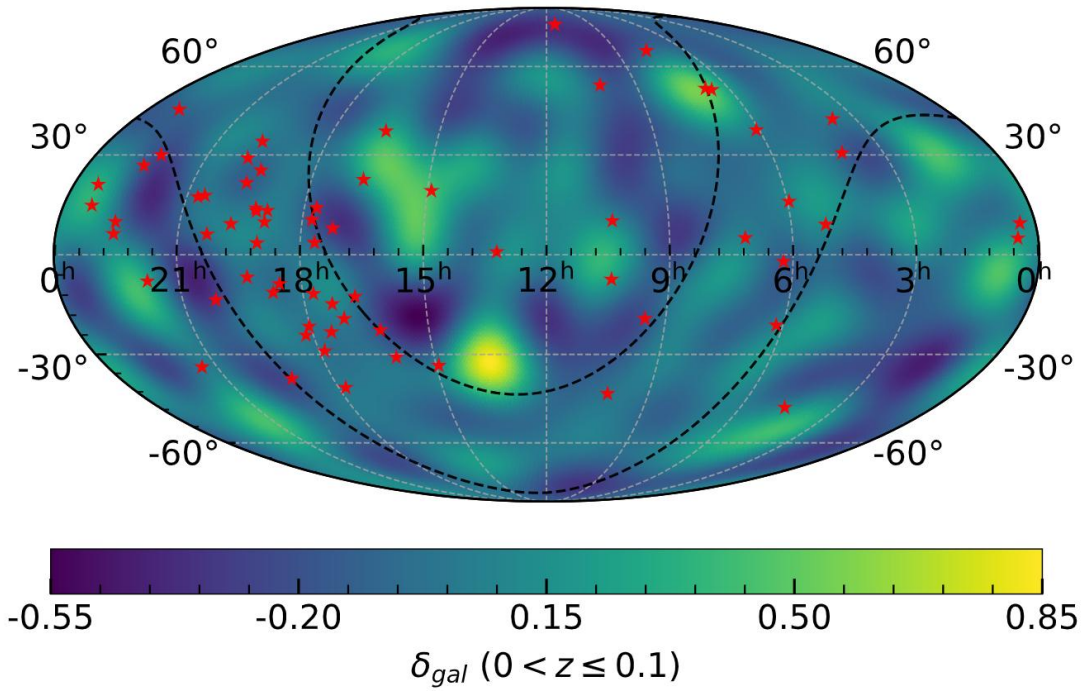
$$\boldsymbol{\theta} \equiv \left(\{a_{\ell 0}\}, \{\mathrm{Re}\, a_{\ell m}\}_{m>0}, \{\mathrm{Im}\, a_{\ell m}\}_{m>0}\right), \qquad -2\ln \pi(\boldsymbol{\theta}) = \boldsymbol{\theta}^{\top} \boldsymbol{\Lambda}\, \boldsymbol{\theta},$$

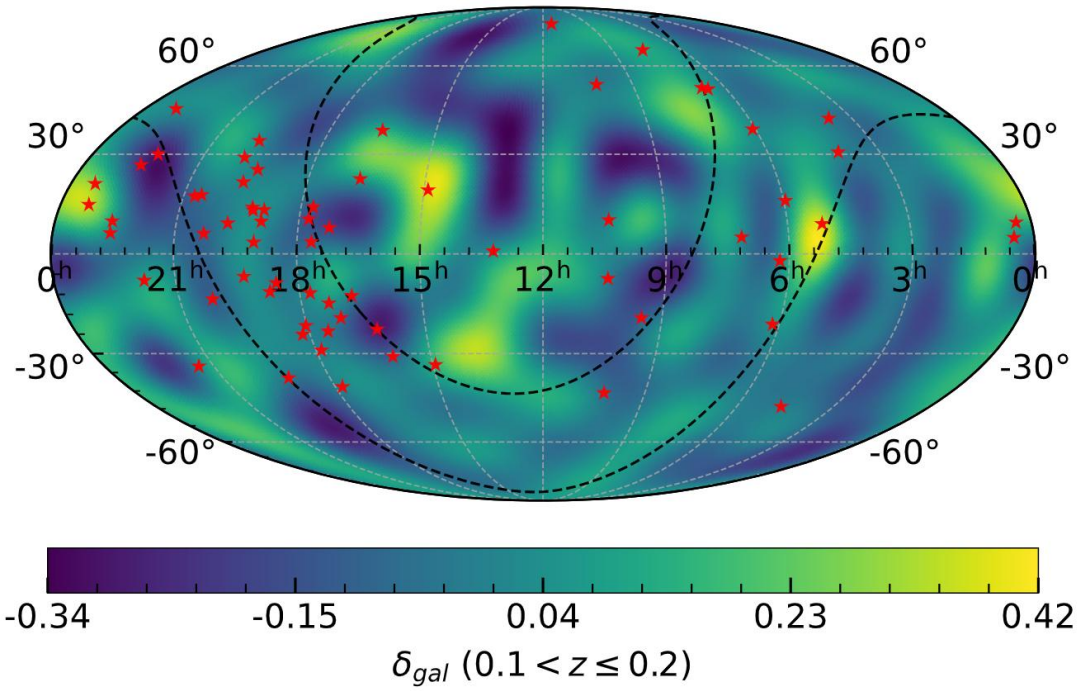
$$\ln \mathcal{L}(\boldsymbol{\theta}) = -\frac{1}{2}(\mathbf{y} - \mathbf{X}\boldsymbol{\theta})^{\top} \mathbf{W} (\mathbf{y} - \mathbf{X}\boldsymbol{\theta}) \qquad \Lambda_{kk} = \begin{cases} 1/C_{\ell}^{\rm target}, & a_{\ell 0}, \\ 2/C_{\ell}^{\rm target}, & \mathrm{Re/Im}\, a_{\ell m}\ (m > 0). \end{cases}$$

by NaMaster *(Hivon et al. 2002; Alonso et al. 2019)*

Reconstructed low-l LSS sky map from 2MPZ galaxy catalog (z<0.2)

(Y. Fang, SCPMA 2026)

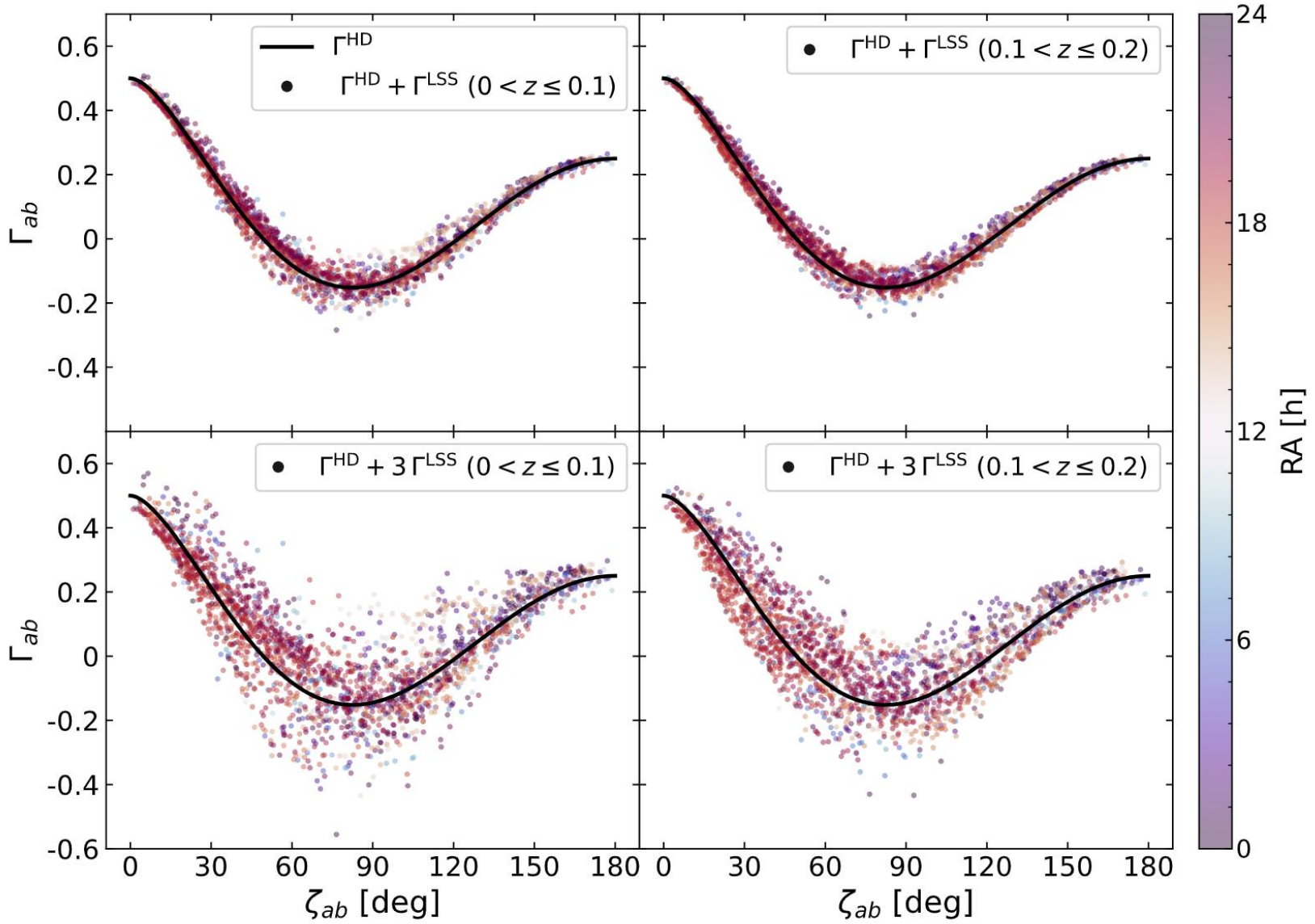




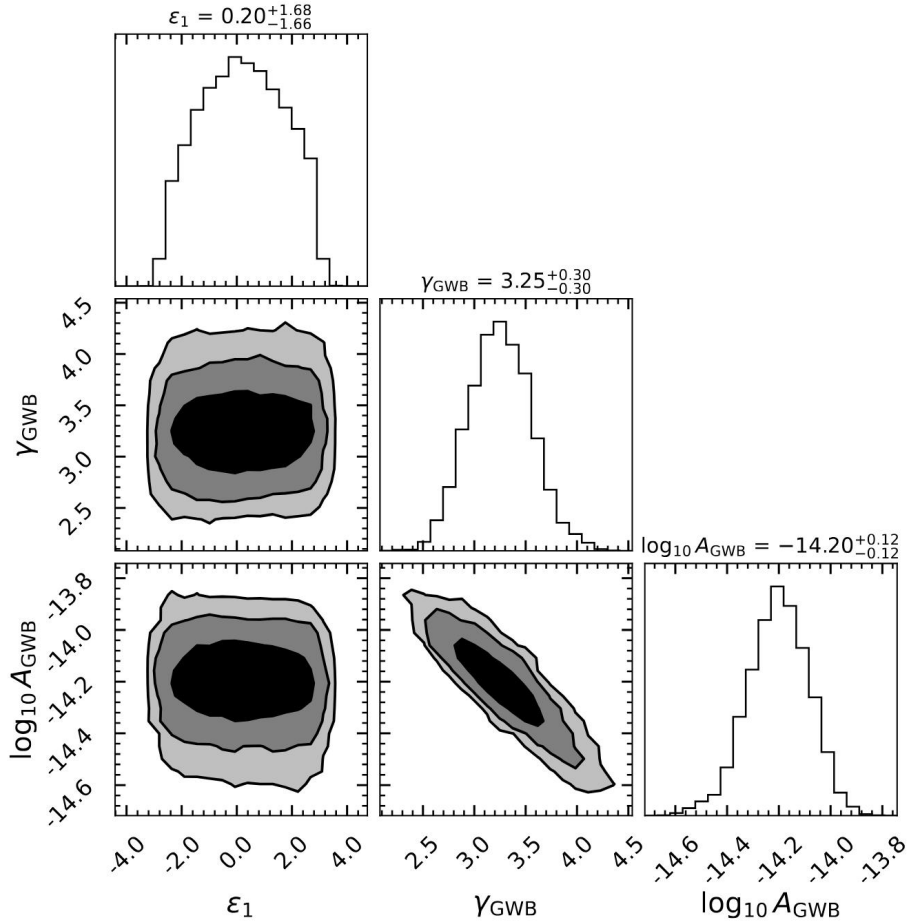
2MPZ: 2MASS Photometric Redshift catalogue (Bilicki et al. 2014)

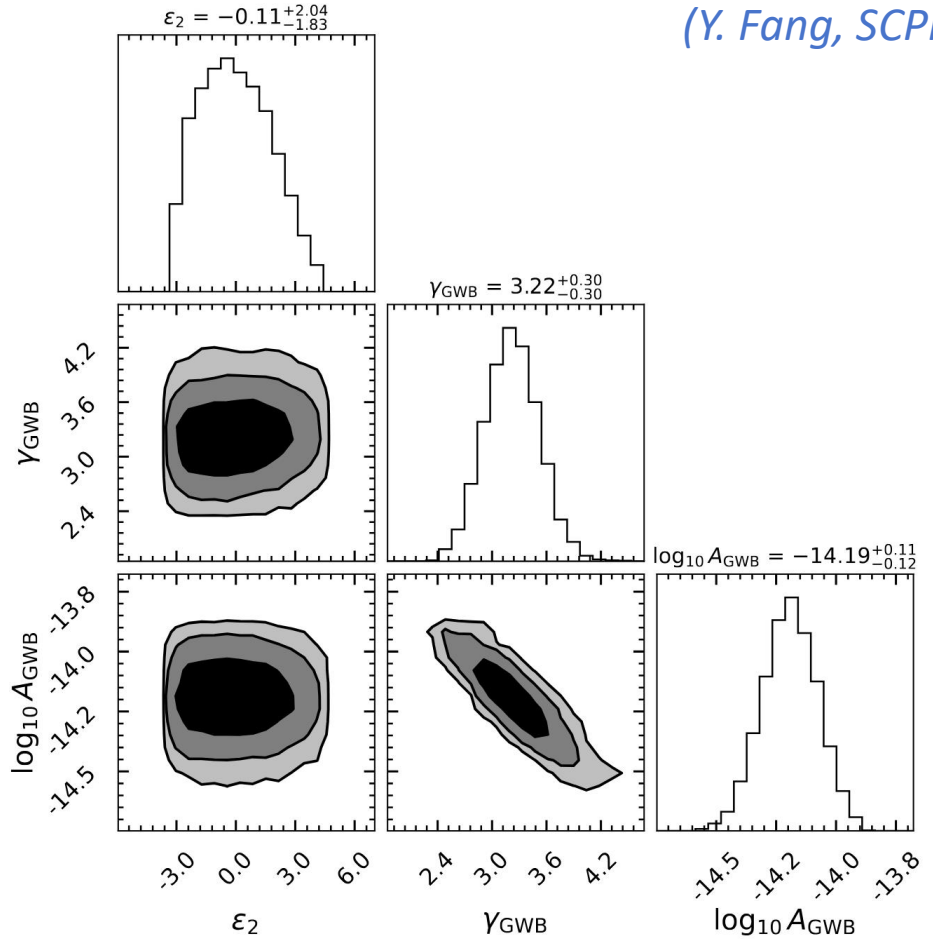
Redshift tomographic LSS-correlated ORF

(Y. Fang, SCPMA 2026)



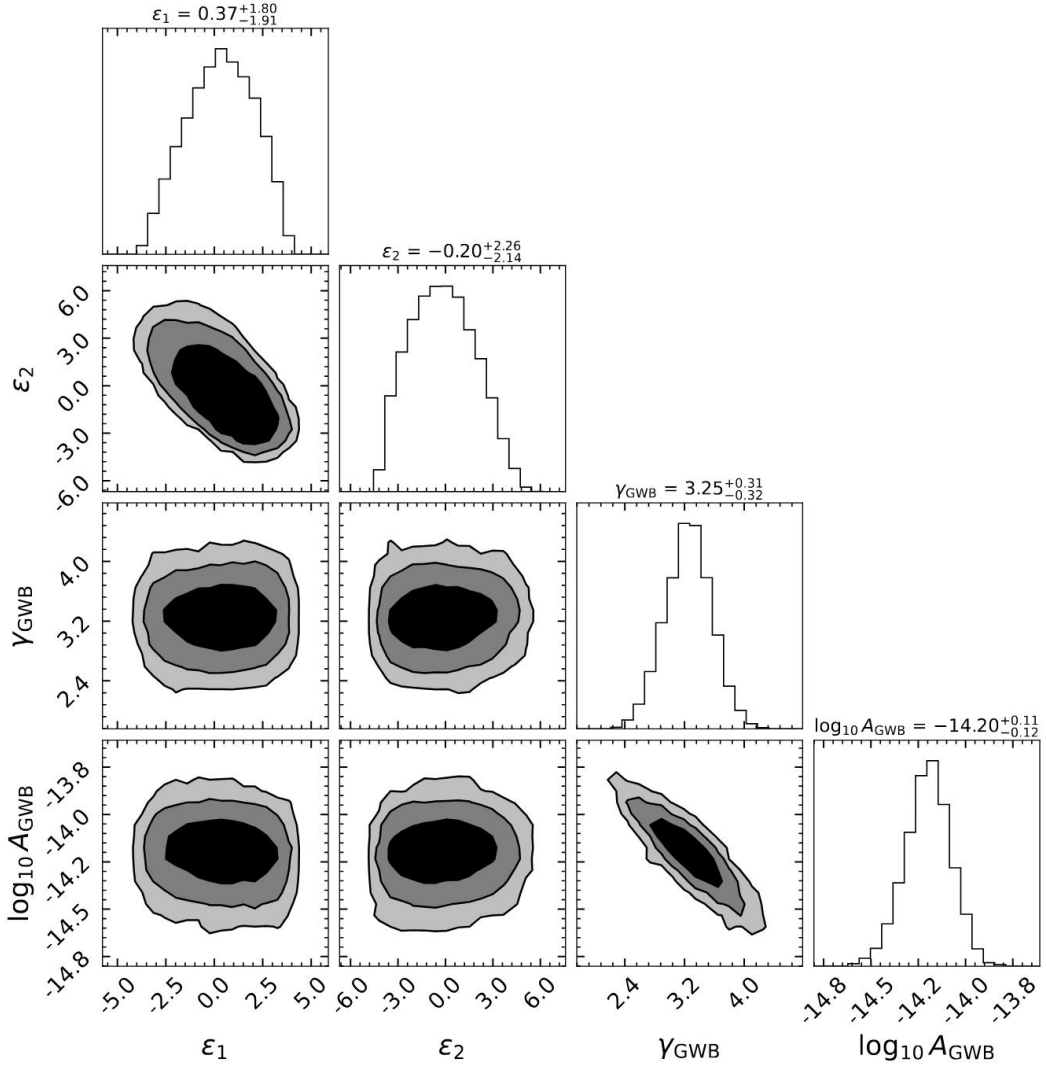
(Y. Fang, SCPMA 2026)

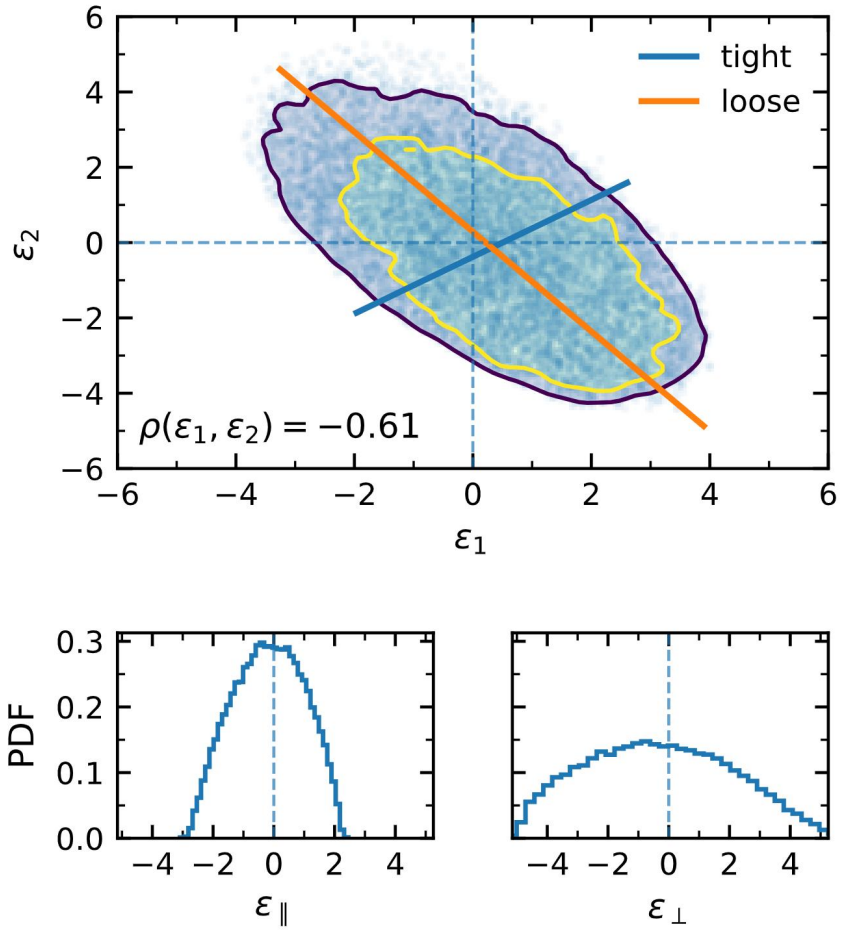




$$\mathcal{B}_{\rm HD+LSS_1,\,HD} = 0.40\,, \qquad \mathcal{B}_{\rm HD+LSS_2,\,HD} = 0.43\,,$$

(Y. Fang, SCPMA 2026)





$$\mathcal{B}_{\rm HD+LSS_1+LSS_2,\,HD} = 0.11$$

Template-based method **VS** cross-map correlation

SNR of LSS-correlated ORF:

(Y. Fang+, in preparation)

$$\rho^2_{\rm matched} = \epsilon^2_{\rm true} \sum_{\ell m} \frac{(a^{\rm LSS}_{\ell m})^2}{\mathcal{B}^2_\ell(N_f, L_{\rm max}) + C^{\rm shot}_\ell}$$

where $\bar{\boldsymbol{a}}^{\rm GW} = \epsilon_{\rm true}\boldsymbol{a}^{\rm LSS}$.

$$\ln \mathcal{L}(\epsilon) = -\frac{1}{2}(\hat{\boldsymbol{a}}^{\rm GW} - \epsilon\boldsymbol{a}^{\rm LSS})^{\intercal}\boldsymbol{\Sigma}^{-1}(\hat{\boldsymbol{a}}^{\rm GW} - \epsilon\boldsymbol{a}^{\rm LSS}) - \frac{1}{2}\ln\det\boldsymbol{\Sigma}$$

where $\boldsymbol{\Sigma} = \boldsymbol{\Sigma}^{\rm PTA} + \boldsymbol{\Sigma}^{\rm shot}$.

$$\Sigma^{\rm PTA}_{\ell m,\ell' m'} = \mathcal{B}^2_\ell \delta_{\ell\ell'}\delta_{mm'}.$$

$$\Sigma^{\rm shot}_{\ell m,\ell' m'} = C^{\rm shot}_\ell \delta_{\ell\ell'}\delta_{mm'}.$$

SNR of SGWB-galaxy cross correlation:

(Cusin+ MNRAS 2025)

$$\left(\frac{S}{N}\right)^2_{\rm GW} = \sum_\ell^{\ell_{\rm max}} \frac{(2\ell+1)(C^{\rm GW\Delta}_\ell)^2}{(C^{\rm GW\Delta}_\ell + N^{\rm GW\Delta,\,tot}_\ell)^2 + (C^{\rm GW}_\ell + N^{\rm GW,\,tot}_\ell)(C^{\Delta}_\ell + N^{\Delta}_{\rm shot})}$$

where

$$C^{\rm GW}_\ell = \frac{2}{\pi}\int {\rm d}k\, k^2\, |\delta\Omega_{{\rm GW},\ell}(k)|^2\,,$$

$$C^{\Delta}_\ell = \frac{2}{\pi}\int {\rm d}k\, k^2\, |\Delta_\ell(k)|^2\,,$$

$$C^{\rm GW\Delta}_\ell = \frac{2}{\pi}\int {\rm d}k\, k^2\, \delta\Omega^*_{{\rm GW},\ell}(k)\,\Delta_\ell(k)\,,$$

Template-based method **VS** cross-map correlation

SNR of LSS-correlated ORF:
(Y. Fang+, in preparation)

$$\rho^2_{\rm matched} = \epsilon^2_{\rm true} \sum_{\ell m} \frac{(a^{\rm LSS}_{\ell m})^2}{\mathcal{B}^2_\ell(N_f, L_{\rm max}) + C^{\rm shot}_\ell}$$

where $\bar{a}^{\rm GW} = \epsilon_{\rm true} a^{\rm LSS}$.

SNR of SGWB-galaxy cross correlation:
(Cusin+ MNRAS 2025)

$$\left(\frac{S}{N}\right)^2_{\rm GW} = \sum_\ell^{\ell_{\rm max}} \frac{(2\ell+1)(C^{\rm GW\Delta}_\ell)^2}{(C^{\rm GW\Delta}_\ell + N^{\rm GW\Delta,\,tot}_\ell)^2 + (C^{\rm GW}_\ell + N^{\rm GW,\,tot}_\ell)(C^{\Delta}_\ell + N^{\Delta}_{\rm shot})}$$

***PTA sensitivity is modeled by N_f and L_{max} (set to 20 here) (preliminary, *Y. Fang+, in preparation*)**

Retained sources	Cusin cross-SNR $N_f = 10$	Template SNR $N_f = 10$	Cusin cross-SNR $N_f \to \infty$	Template SNR $N_f \to \infty$
All sources	0.00086042	0.03135253	0.00086042	0.03140692
$h_{eff} < 10^{-15}$	0.68883031	0.57825751	0.79420189	1.26550580
$h_{eff} < 10^{-16}$	1.43347375	0.60357315	3.88860323	5.30233439

Conclusion

Method. We proposed the first Bayesian search for LSS-correlated SGWB anisotropy that incorporates an ORF template (projected from galaxy map) directly into the PTA likelihood.

Observations. The NANOGrav 15-year data show no evidence for anisotropy correlated with the 2MPZ galaxy distribution at $z < 0.2$.

Template sensitivity. In simulated SGWB realizations with simplified PTA sensitivity, the ORF template-based search and map-based cross-correlation yield comparable SNRs after bright-source removal.

The template-based method is a promising tool for future PTA searches for LSS-correlated anisotropy or other physically motivated anisotropy patterns.